

Thermomechanical interactions due to laser pulse in microstretch thermoelastic medium

R. KUMAR¹⁾, A. KUMAR²⁾, D. SINGH³⁾

¹⁾*Department of Mathematics
Kurukshetra University Kurukshetra
Haryana, India
e-mail: rajneesh_kuk@rediffmail.com*

²⁾*Department of Mathematics
Punjab Technical University
Jalandhar, Punjab, India
e-mail: arvi.math@gmail.com*

³⁾*Guru Nanak Dev Engineering College
Ludhiana, Punjab, India*

THE PRESENT INVESTIGATION DEALS WITH deformation in microstretch generalized thermoelastic medium subjected to thermomechanical loading induced by thermal laser pulse. The Laplace and Fourier transform techniques are used to solve the problem, and concentrated normal force and thermal source describe the application of this approach. The closed form expressions of normal stress, tangential stress, couple stress, microstress and temperature distribution are obtained for the transferred domain. The numerical inversion technique of Laplace transform and Fourier transform has been applied to obtain the resulting quantities in the physical domain after developing a computer program. Normal stress, tangential stress, coupled stress and microstress temperature distribution are depicted graphically to show the microstretch effect. Some particular and special cases of interest are gathered and presented in the investigation.

Key words: microstretch thermoelastic, integral transform, pulse laser, concentrated normal force and concentrated thermal source.

Copyright © 2015 by IPPT PAN

Introduction

MODERN ENGINEERING STRUCTURES such as polycrystalline materials, materials with fibrous or coarse grain structure are often made from materials possessing internal structure. The classical theory of elasticity is inadequate in describing the behavior of such materials. The analysis of such materials requires incorporating the theory of oriented media. The linear theory of micropolar elasticity was developed by ERINGEN [1] to describe deformation of elastic media with ori-

ented particles. A micropolar continuum is a collection of interconnected particles in the form of small rigid bodies undergoing both translational and rotational motions. Typical examples of such materials are granular media and multimolecular bodies whose microstructures act as an evident part in their macroscopic responses. Rigid chopped fibers, elastic solids with rigid granular inclusions and other industrial materials such as liquid crystals are examples of such materials.

ERINGEN [2] extended his work to include the effect of axial stretch during the rotation of molecules and developed the theory of micropolar elastic solid with stretch. The material points in this continuum possess not only classical translational degrees of freedom represented by the deformation vector field but also intrinsic rotations and an intrinsic axial stretch. The difference between these solids and micropolar elastic solids stems from the presence of scalar microstretch and a vector's first moment. ERINGEN [3] developed the theory of thermomicrostretch elastic solids. Eringen [3] also derived the equations of motions, constitutive equations and boundary conditions for thermomicrostretch fluids, and obtained the solution to the problem of acoustical waves in bubbly liquids. Microstretch continuum is a model for Bravais lattice with the basis on the atomic level and two phase dipolar solids with a core on the macroscopic level. Composite materials reinforced with chopped elastic fibers, porous media whose pores are filled with gas or in viscid liquid, asphalt or other elastic inclusions and solid-liquid crystals, etc. are examples of microstretch solids.

CICCO [4] discussed stress concentration effects in microstretch elastic bodies. EZZAT and AWAD [5] adopted the normal mode analysis technique to obtain the temperature gradient, displacement, stresses and microrotation. The fundamental solution in the theory of thermomicrostretch elastic diffusive solids was developed by KUMAR and KANSAL [6]. A domain of influence theorem for microstretch elastic materials was investigated by MARIN [7]. Thermomechanical interactions in generalized thermomicrostretch elastic half space were discussed by AOUADI [8]. The gravitational effect on plane waves in generalized thermomicrostretch elastic solid under Green–Naghdi theory was studied by OTHMAN *et al.* [9].

Laser technology has a vital application in testing and evaluation of nondestructive materials. When a solid is heated with a laser pulse, it absorbs some energy, which results in an increase in localized temperature. This causes thermal expansion and generation of ultrasonic waves in the material. The irradiation of the surface of a solid by pulsed laser light generates wave motion in the solid material. There are generally two mechanisms for such wave generation, depending on the energy density deposited by the laser pulse. At high energy density a thin surface layer of the solid material melts, followed by an ablation process whereby particles fly off the surface, thus giving rise to forces that generates ultrasonic waves. At low energy density, the surface material does not melt, but it expands

at a high rate and wave and wave motion are generated due to thermoelastic processes.

Very rapid thermal processes (e.g., thermal shock due to exposure to an ultra-short laser pulse) are interesting from the standpoint of thermoelasticity, since they require a coupled analysis of the temperature and deformation fields. A thermal shock induces very rapid movement in structural elements, giving rise to very significant inertial forces, and thereby, to an increase in vibration. Rapidly oscillating contraction and expansion generates temperature changes in materials susceptible to diffusion of heat by conduction [10]. This mechanism has attracted considerable attention due to the extensive use of pulsed laser technologies in material processing, and nondestructive testing and characterization of material properties [11, 12]. The so-called ultrashort lasers are those with pulse durations ranging from nanoseconds to femtoseconds. In the case of ultrashort pulsed laser heating, high intensity energy flux and ultrashort duration may lead to very large thermal gradients or ultra-high heating at the boundaries. In such cases, as it was pointed out by many researchers, the classical Fourier model, which leads to an infinite propagation speed of thermal energy, is no longer valid [13]. Researchers have proposed several models to describe the mechanism of heat conduction during short-pulse laser heating, such as the parabolic one-step model [14], the hyperbolic one-step model [15], and the parabolic two-step and hyperbolic two-step models [16, 17]. It has been found that the microscopic two-step models, i.e., parabolic and hyperbolic two-step models, are usually useful for thin films. Simulation of laser ultrasound waveform in nonmetallic materials was discussed by WANG *et al.* [18].

SCRUBY *et al.* [19] considered the point source model to study the ultrasonic generation by lasers. He studied the surface heated by laser pulse irradiation in the thermoelastic system as a surface center of expansion (SCOE). He also discussed the applications of laser technology in flaw detection and acoustic microscopy. ROSE [20] later presented a more exact mathematical basis. The point source model explains the main features of laser-generated ultrasound waves but it fails to explain the precursor in epicenter waves. Later introducing thermal diffusion, McDONALD [21] and SPICER [22] proposed a new model known as laser-generated ultrasound model. This model reported excellent agreement between theory and experiment for metallic materials. But due to the optical penetration effect, this model cannot be applied to the study of laser-generated ultrasound in nonmetallic materials directly. The optical absorption occurs at the surface layer in metallic materials, and the heat penetration is a result of heat diffusion. In nonmetallic materials, the laser beam can penetrate the specimen to some finite depth and induce a buried bulk-thermal source, so features of the laser-generated ultrasound are significantly different from those in metallic materials.

DUBOIS [23] experimentally demonstrated that the penetration depth plays a very important role in the laser-ultrasound generation process. EZZAT *et al.* [24] discussed thermoelastic behavior in metal films induced by fractional ultrafast laser. AL-HUNITI and AL-NIMR [25] investigated the thermoelastic behavior of a composite slab under rapid dual-phase lag heating. The comparison of one-dimensional and two-dimensional axisymmetric approaches to the thermo-mechanical response caused by ultrashort laser heating was studied by CHEN *et al.* [26]. KIM *et al.* [27] studied thermoelastic stresses in a bonded layer due to pulsed laser radiation. Thermoelastic material response due to laser pulse heating in the context of four theorems of thermoelasticity was discussed by YOUSSEF and AL-BARY [28]. The theoretical study of the effect of enamel parameters on laser induced surface acoustic waves in human incisor was carried out by YUAN *et al.* [29]. A two-dimensional generalized thermoelastic diffusion problem for a thick plate under the effect of laser pulse thermal heating was studied by ELHAGARY [30].

In this research, taking into account the microstretch effect and radiation of ultrashort laser, we established a model for a microstretch thermoelastic medium by using Laplace and Fourier transforms. The stress components and temperature distribution were computed numerically. The resulting expressions were then applied to the problem of a microstretch thermoelastic medium whose boundary is subjected to two types of loads: mechanical load and thermal load. The resulting quantities are presented graphically to show the effect of microstretch and temperature.

1. Basic equations

Following ERINGEN [31], LORD and SHULMAN [32] and GREEN and LINDSAY [33], the basic equations for homogeneous, isotropic microstretch generalized thermoelastic solids in the absence of body forces, body couples and stretch forces are given by

$$(1.1) \quad (\lambda + \mu)\nabla(\nabla \cdot \mathbf{u}) + (\mu + K)\nabla^2 \mathbf{u} + K\nabla \times \boldsymbol{\phi} + \lambda_0 \nabla \phi^* - \beta_1 \left(1 + \tau_1 \frac{\partial}{\partial t}\right) \nabla T = \rho \ddot{\mathbf{u}},$$

$$(1.2) \quad (\gamma \nabla^2 - 2K)\boldsymbol{\phi} + (\alpha + \beta)\nabla(\nabla \cdot \boldsymbol{\phi}) + K\nabla \times \mathbf{u} = \rho j \ddot{\boldsymbol{\phi}},$$

$$(1.3) \quad (\alpha_0 \nabla^2 - \lambda_1)\phi^* - \lambda_0 \nabla \cdot \mathbf{u} + \nu_1 \left(1 + \tau_1 \frac{\partial}{\partial t}\right) T = \frac{\rho j_0}{2} \ddot{\phi}^*,$$

$$(1.4) \quad K^* \nabla^2 T = \rho c^* \left(\frac{\partial}{\partial t} + \tau_0 \frac{\partial^2}{\partial t^2}\right) T + \left(1 + \varepsilon \tau_0 \frac{\partial}{\partial t}\right) (\beta_1 T_0 \nabla \cdot \dot{\mathbf{u}} - \rho Q) \\ + \nu_1 T_0 \left(\frac{\partial}{\partial t} + \varepsilon \tau_0 \frac{\partial^2}{\partial t^2}\right) \phi^*,$$

$$(1.5) \quad t_{ij} = (\lambda_0 \phi^* + \lambda u_{r,r}) \delta_{ij} + \mu(u_{i,j} + u_{j,i}) + K(u_{j,i} - \epsilon_{ijk} \phi_k) - \beta_1 \left(1 + \tau_1 \frac{\partial}{\partial t}\right) \delta_{ij} T,$$

$$(1.6) \quad m_{ij} = \alpha\phi_{r,r}\delta_{ij} + \beta\phi_{i,j} + \gamma\phi_{j,i} + b_0\epsilon_{mji}\phi_{,m}^*,$$

$$(1.7) \quad \lambda_i^* = \alpha_0\phi_{,i}^* + b_0\epsilon_{ijm}\phi_{j,m}.$$

The plate surface is illuminated by laser pulse given by the following heat input:

$$(1.8) \quad Q = I_0 f(t) g(x_1) h(x_3),$$

where I_0 is the energy absorbed. The temporal profile $f(t)$ is represented as

$$(1.9) \quad f(t) = \frac{t}{t_0^2} e^{-\left(\frac{t}{t_0}\right)}.$$

Here t_0 is the pulse rise time. The pulse is also assumed to have a Gaussian spatial profile in x_1

$$(1.10) \quad g(x) = \frac{1}{2\pi r^2} e^{-\left(\frac{x_1^2}{r^2}\right)},$$

where r is the beam radius, and as a function of the depth x_3 , the heat deposition due to the laser pulse is assumed to decay exponentially within the solid:

$$(1.11) \quad h(x_3) = \gamma^* e^{-\gamma^* x_3}.$$

Equation (1.8) with the aid of Eqs. (1.9)–(1.11) takes the form

$$(1.12) \quad Q = \frac{I_0 \gamma^*}{2\pi r^2 t_0^2} t e^{-\left(\frac{t}{t_0}\right)} e^{-\left(\frac{x_1^2}{r^2}\right)} e^{-\gamma^* x_3},$$

where λ , μ , α , β , γ , K , λ_0 , λ_1 , α_0 , b_0 , are material constants, ρ is mass density, $\mathbf{u} = (u_1, u_2, u_3)$ is the displacement vector and $\mathbf{\Phi} = (\phi_1, \phi_2, \phi_3)$ is the microrotation vector, ϕ^* is the scalar microstretch function, T is temperature and T_0 is the reference temperature of the body chosen, K^* is the coefficient of thermal conductivity, c^* is the specific heat at constant strain, j is the microinertia, $\beta_1 = (3\lambda + 2\mu + K)\alpha_{t1}$, $\nu_1 = (3\lambda + 2\mu + K)\alpha_{t2}$, α_{t1} , α_{t2} are the coefficients of linear thermal expansion, j_0 is the microinertia for the microelements, t_{ij} are the components of stress, m_{ij} are the components of couple stress, λ_i^* is the microstress tensor, δ_{ij} is the Kroneker delta function, and τ_0, τ_1 are thermal relaxation times with $\tau_0 \geq \tau_1 \geq 0$. Here $\tau_0 = \tau_1 = \gamma_1 = 0$ for coupled thermoelastic theory (CT) model, $\tau_1 = 0$, $\epsilon = 1$ for Lord–Shulman (LS) model [27] and $\epsilon = 0$, where $\tau^0 > 0$ for Green–Lindsay (GL) model [28].

In the above equations, the symbol (“,”) followed by a suffix denotes differentiation with respect to spatial coordinates and a superposed dot (“’”) denotes the derivative with respect to time.

2. Formulation of the problem

We consider a rectangular Cartesian coordinate system $OX_1X_2X_3$ having origin on x_3 -axis with the x_3 -axis pointing vertically downward the medium. A normal force/thermal source is assumed to act at the origin of the rectangular Cartesian coordinate system.

We consider the plane strain problem with all the field variables depending on (x_1, x_3, t) . For two dimensional problems, we use

$$(2.1) \quad \mathbf{u} = (u_1, 0, u_3), \quad \boldsymbol{\phi} = (0, \phi_2, 0).$$

For further consideration, it is convenient to introduce in Eq. (1.1)–(1.4) the dimensionless quantities defined as

$$(2.2) \quad \begin{aligned} x'_i &= \frac{\omega^*}{c_1} x_i, & u'_i &= \frac{\rho\omega^*c_1}{\beta_1T_0} u_i, & \phi'_i &= \frac{\rho c_1^2}{\beta_1T_0} \phi_i, & \phi^{*'} &= \frac{\rho c_1^2}{\beta_1T_0} \phi^*, \\ T' &= \frac{T}{T_0}, & t' &= \omega^* t, & \tau'_1 &= \omega^* \tau_1, & \tau'_0 &= \omega^* \tau_0, & t'_{ij} &= \frac{1}{\beta_1T_0} t_{ij}, \\ \omega^* &= \frac{\rho c_1^2}{K^*}, & c_1^2 &= \frac{\lambda + 2\mu + k}{\rho}, & m_{ij}^* &= \frac{\omega^*}{c\beta_1T_0} m_{ij}, & Q' &= \frac{\beta_1^2}{\rho c_1^2}. \end{aligned}$$

Making use of Eq. (2.2) in Eqs. (1.1)–(1.3) and with the aid of Eq. (2.1), we obtain:

$$(2.3) \quad a_1 \frac{\partial e}{\partial x_1} + a_2 \nabla^2 u_1 - a_3 \frac{\partial \phi_2}{\partial x_3} + a_4 \frac{\partial \phi^*}{\partial x_1} - \left(1 + \tau_1 \frac{\partial}{\partial t}\right) \frac{\partial T}{\partial x_1} = \ddot{u}_1,$$

$$(2.4) \quad a_1 \frac{\partial e}{\partial x_3} + a_2 \nabla^2 u_3 + a_3 \frac{\partial \phi_2}{\partial x_1} + a_4 \frac{\partial \phi^*}{\partial x_3} - \left(1 + \tau_1 \frac{\partial}{\partial t}\right) \frac{\partial T}{\partial x_3} = \ddot{u}_3,$$

$$(2.5) \quad \nabla^2 \phi_2 - 2a_6 \phi_2 + a_6 \left(\frac{\partial u_1}{\partial x_3} - \frac{\partial u_3}{\partial x_1} \right) = a_7 \ddot{\phi}_2,$$

$$(2.6) \quad \nabla^2 \phi^* - a_8 \phi^* - a_9 e + a_{10} \left(1 + \tau_1 \frac{\partial}{\partial t}\right) T = a_{12} \ddot{\phi}^*,$$

$$(2.7) \quad -\nabla^2 T + \left(\frac{\partial}{\partial t} + \tau_0 \frac{\partial^2}{\partial t^2}\right) T + a_{13} \left(\frac{\partial}{\partial t} + \varepsilon \tau_0 \frac{\partial^2}{\partial t^2}\right) e + a_{14} \left(\frac{\partial}{\partial t} + \varepsilon \tau_0 \frac{\partial^2}{\partial t^2}\right) \phi^* \\ = Q_0 f^*(x_1, t) e^{-\gamma^* x_3}.$$

Here,

$$\begin{aligned} a_1 &= \frac{\lambda + \mu}{\rho c_1^2}, & a_2 &= \frac{\mu + K}{\rho c_1^2}, & a_3 &= \frac{K}{\rho c_1^2}, & a_4 &= \frac{\lambda_0}{\rho c_1^2}, & a_6 &= \frac{K c_1^2}{\gamma \omega^{*2}}, \\ a_7 &= \frac{\rho j c_1^2}{\gamma}, & a_8 &= \frac{\lambda_1 c_1^2}{\alpha_0 \omega^{*2}}, & a_9 &= \frac{\lambda_0 c_1^2}{\alpha_0 \omega^{*2}}, & a_{10} &= \frac{v_1 \rho c_1^4}{\beta_1 \alpha_0 \omega^{*2}}, \\ a_{12} &= \frac{\rho c_1^2 j_0}{2\alpha_0}, & a_{13} &= \frac{\beta_1 T_0^2}{\rho \omega^* K^*}, & a_{14} &= \frac{v_1 \beta_1 T_0}{\omega^* \rho K^*}, & Q_0 &= \frac{a_{13} \rho I_0 \gamma^*}{2\pi r^2 t_0^2}, \end{aligned}$$

$$f(x_1, t) = \left[t + \varepsilon\tau_0 \left(1 - \frac{t}{t_0} \right) \right] e^{-\left(\frac{x_1^2}{r^2} + \frac{t}{t_0}\right)}.$$

$\nabla^2 = \frac{\partial^2}{\partial x_1^2} + \frac{\partial^2}{\partial x_3^2}$, is the Laplacian operator.

The displacement components u_1 and u_3 are related to the non-dimensional potential functions ϕ and ψ as

$$(2.8) \quad u_1 = \frac{\partial\phi}{\partial x_1} - \frac{\psi}{\partial x_3}, \quad u_3 = \frac{\partial\phi}{\partial x_3} + \frac{\psi}{\partial x_1}.$$

Substituting the values of u_1 and u_3 from Eq. (2.8) into Eqs. (2.3)–(2.7) and with the aid of Eq. (2.1), we obtain:

$$(2.9) \quad \nabla^2\phi - \ddot{\phi} + a_4\phi^* - \left(1 + \tau_1 \frac{\partial}{\partial t} \right) T = 0,$$

$$(2.10) \quad \left(\nabla^2 - a_8 - a_{12} \frac{\partial^2}{\partial t^2} \right) \phi^* - a_9 \nabla^2\phi + a_{10} \left(1 + \tau_1 \frac{\partial}{\partial t} \right) T = 0,$$

$$(2.11) \quad \left(1 + \tau_0 \frac{\partial}{\partial t} \right) \dot{T} + a_{13} \left(\frac{\partial}{\partial t} + \varepsilon\tau_0 \frac{\partial^2}{\partial t^2} \right) \nabla^2\phi + a_{14} \left(1 + \varepsilon\tau_0 \frac{\partial}{\partial t} \right) \dot{\phi}^* - \nabla^2 T = Q_0 f^*(x_1, t) e^{-\gamma^* x_3},$$

$$(2.12) \quad a_2 \nabla^2\psi - \ddot{\psi} + a_3\phi_2 = 0,$$

$$(2.13) \quad \nabla^2\phi_2 - 2a_6\phi_2 - a_6 \nabla^2\psi = a_7 \ddot{\phi}_2.$$

3. Solution of the problem

We define Laplace transform and Fourier transform respectively as

$$(3.1) \quad \bar{f}(s, x_1, x_3) = \int_0^\infty f(t, x_1, x_3) e^{-st} dt,$$

$$(3.2) \quad \hat{f}(x_3, \xi, s) = \int_{-\infty}^\infty \bar{f}(s, x_1, x_3) e^{i\xi x_1} dx_1.$$

Applying the Laplace transform defined by Eq. (3.1) to Eqs. (2.9)–(2.13) and then applying Fourier transforms defined by (3.2) to the resulting quantities, we obtain the following:

$$(3.3) \quad \left(\frac{d^2}{dx^2} - \xi^2 \right) \hat{\phi} + a_4 \widehat{\phi^*} - \tau_{11} \hat{T} = 0,$$

$$(3.4) \quad -a_9 \left(\frac{d^2}{dx^2} - \xi^2 \right) \hat{\phi} + \left(\frac{d^2}{dx^2} - a_{20} \right) \widehat{\phi^*} + a_{21} \hat{T} = 0,$$

$$(3.5) \quad a_{22} \left(\frac{d^2}{dx^2} - \xi^2 \right) \hat{\phi} + a_{23} \widehat{\phi}^* - \left(\frac{d^2}{dx^2} - a_{33} \right) \hat{T} = Q_1 e^{-\gamma^* x_3},$$

$$(3.6) \quad \left[\frac{d^2}{dx_3^2} - \xi^2 - s^2 \right] \widehat{\psi} - a_3 \widehat{\phi}_2 = 0,$$

$$(3.7) \quad \left[\frac{d^2}{dx_3^2} - a_{30} \right] \widehat{\phi}_2 + a_6 \left[\frac{d^2}{dx_3^2} - \xi^2 \right] \widehat{\psi} = 0.$$

Eliminating $\widehat{\phi}^*$ and \hat{T} , $\hat{\phi}$ and \hat{T} , and $\hat{\phi}$ and $\widehat{\phi}^*$ respectively from equations (3.3)–(3.5), we obtain:

$$(3.8) \quad [D^6 - AD^4 - BD^2 + C] \hat{\phi} = f_1 e^{-\gamma^* x_3},$$

$$(3.9) \quad [D^6 - AD^4 - BD^2 + C] \widehat{\phi}^* = f_2 e^{-\gamma^* x_3},$$

$$(3.10) \quad [D^6 - AD^4 - BD^2 + C] \hat{T} = f_3 e^{-\gamma^* x_3},$$

Also, eliminating ϕ_2 from equations (3.6)–(3.7) yields

$$(3.11) \quad [D^4 + ED^2 + F] \widehat{\psi} = 0,$$

where

$$\begin{aligned} A &= (a_{22}\tau_{11} + a_{33} + a_{28}), & B &= a_{22}(a_{25} - \tau_{11}\xi^2) + a_{23}a_{26} - a_{33}a_{28} - a_{29}, \\ C &= -a_{22}a_{25}\xi^2 + a_{23}a_{27} + a_{33}a_{29}, & E &= \frac{a_{31}}{a_2}, & F &= \frac{a_{32}}{a_2}, & \tau_{11} &= (1 + \tau_1 s), \\ \xi_1 &= \xi^2 + s^2, & f_1 &= -Q_1(\tau_{11}\gamma^{*2} + a_{25}), & f_2 &= -Q_1(a_{26}\gamma^{*2} + a_{27}), \\ f_3 &= -Q_1(\gamma^{*4} - a_{28}\gamma^{*2} + a_{29}), & f_4 &= [\gamma^{*6} - A\gamma^{*4} - B\gamma^{*2} + C] \end{aligned}$$

and

$$\begin{aligned} a_{20} &= (\xi^2 + a_8 + s^2 a_{12}), & a_{21} &= a_{10}\tau_{11}, & a_{22} &= a_{13}(s + \varepsilon s^2 \tau_0), \\ a_{23} &= a_{14}(s + \varepsilon s^2 \tau_0), & a_{24} &= \xi^2 - s - s^2 \tau_0, & a_{25} &= a_4 a_{21} - a_{20} \tau_1, \\ a_{26} &= a_9 \tau_{11} - a_{21}, & a_{27} &= a_{21} \xi_1 - \xi^2 \tau_{11} a_9, & a_{28} &= \xi_1 + a_{20} - a_4 a_9, \\ a_{29} &= \xi_1 a_{20} - a_4 a_9 \xi^2, & a_{30} &= \xi^2 + 2a_6 + s^2 a_7, & a_{31} &= a_3 a_6 - a_2 a_{30} - a_2 \xi_1, \\ a_{32} &= -a_3 a_6 \xi^2 + a_2 a_{30} \xi_1, & a_{33} &= \xi^2 + s + s^2 \tau_0. \end{aligned}$$

The solutions to Eqs. (3.8)–(3.11) satisfying the radiation conditions $(\hat{\phi}, \widehat{\phi}^*, \hat{T}, \widehat{\phi}_2, \widehat{\psi}) \rightarrow 0$ as $x_3 \rightarrow \infty$ are given by

$$(3.12) \quad \hat{\phi} = B_1 e^{-m_1 x_3} + B_2 e^{-m_2 x_3} + B_3 e^{-m_3 x_3} + L_1 e^{-\gamma^* x_3},$$

$$(3.13) \quad \widehat{\phi}^* = d_1 B_1 e^{-m_1 x_3} + d_2 B_2 e^{-m_2 x_3} + d_3 B_3 e^{-m_3 x_3} + L_2 e^{-\gamma^* x_3},$$

$$(3.14) \quad \hat{T} = e_1 B_1 e^{-m_1 x_3} + e_2 B_2 e^{-m_2 x_3} + e_3 B_3 e^{-m_3 x_3} + L_3 e^{-\gamma^* x_3},$$

$$(3.15) \quad \widehat{\psi} = B_4 e^{-m_4 x_3} + B_5 e^{-m_5 x_3},$$

$$(3.16) \quad \widehat{\phi}_2 = h_4 B_4 e^{-m_4 x_3} + h_5 B_5 e^{-m_5 x_3},$$

where

$$d_i = \frac{a_{26} m_i^2 + a_{27}}{\tau_{11} m_i^2 + a_{25}}, \quad e_i = \frac{m_i^4 - a_{28} m_i^2 + a_{29}}{\tau_{11} m_i^2 + a_{25}},$$

$$L_i = \frac{f_i}{[m_i^6 - A m_i^4 - B m_i^2 + C]}, \quad i = 1, 2, 3$$

and

$$h_l = \frac{a_2(m_l^2 - \xi_1)}{a_3}, \quad l = 4, 5$$

and m_i^2 ($i = 1, 2, 3$) are the roots of the characteristic equation of Eq. (3.8) and m_l^2 ($l = 4, 5$) are the roots of the characteristic equation of Eq. (3.11).

4. Boundary conditions

We consider concentrated normal force and concentrated thermal source at the boundary surface $x_3 = 0$; mathematically, these can be written as

$$(4.1) \quad t_{33} = -F_1 \delta(x_1) \delta(t), \quad t_{31} = 0, \quad m_{32} = 0, \quad \lambda_3^* = 0, \quad T = F_2 \delta(x_1) \delta(t),$$

where F_1 is the magnitude of the applied force and F_2 is the constant temperature applied at the boundary.

Case 1 is for the normal force $F_2 = 0$;

Case 2 is for the thermal source $F_1 = 0$.

Substituting the values of $\widehat{\phi}$, $\widehat{\phi}^*$, \widehat{T} , $\widehat{\psi}$, $\widehat{\phi}_2$ from Eqs. (3.12)–(3.16) into the boundary condition (4.1), and using Eqs. (1.5)–(1.7), (2.1)–(2.2), (3.1)–(3.2) and solving the resulting equations, we obtain:

$$(4.3) \quad \widehat{t}_{33} = \sum_{i=1}^5 G_{1i} e^{-m_i x_3} + M_1 e^{-\gamma^* x_3},$$

$$(4.4) \quad \widehat{t}_{31} = \sum_{i=1}^5 G_{2i} e^{-m_i x_3} + M_2 e^{-\gamma^* x_3},$$

$$(4.5) \quad \widehat{m}_{32} = \sum_{i=1}^5 G_{3i} e^{-m_i x_3} + M_3 e^{-\gamma^* x_3},$$

$$(4.6) \quad \widehat{\lambda}_3^* = \sum_{i=1}^5 G_{4i} e^{-m_i x_3} + M_4 e^{-\gamma^* x_3},$$

$$(4.7) \quad \hat{T} = \sum_{i=1}^5 G_{5i} e^{-m_i x_3} + M_5 e^{-\gamma^* x_3},$$

where

$$G_{mi} = g_{mi} C_i, \quad C_i = \frac{\Delta_i}{\Delta_0}, \quad i = 1, 2, \dots, 5;$$

also,

$$\begin{aligned} g_{1i} &= b_1 \alpha_{1i} + b_2 (m_i^2 - \xi^2) + b_3 m_i^2 - \tau_{11} \alpha_{2i}, \\ g_{2i} &= -\iota b_3 \xi m_i, \quad g_{3i} = \iota b_9 \xi \alpha_{1i}, \\ g_{4i} &= -\alpha_0 b_{10} m_i \alpha_{1i}, \quad g_{5i} = \alpha_{2i}, \quad i = 1, 2, 3 \end{aligned}$$

and

$$\begin{aligned} g_{1l} &= \iota b_3 \xi m_l, & g_{2l} &= b_6 m_l^2 + b_5 \xi^2 - b_7 \alpha_{3l}, \\ g_{3l} &= -b_8 \alpha_{3l} m_l, & g_{4l} &= -\iota \xi b_0 b_{10} \alpha_{3l}, \quad g_{5l} = 0, \quad l = 4, 5, \end{aligned}$$

$$\Delta_0 = \begin{vmatrix} g_{11} & g_{12} & g_{13} & g_{14} & g_{15} \\ g_{21} & g_{22} & g_{23} & g_{24} & g_{25} \\ g_{31} & g_{32} & g_{33} & g_{34} & g_{35} \\ g_{41} & g_{42} & g_{43} & g_{44} & g_{45} \\ \alpha_{21} & \alpha_{22} & \alpha_{23} & 0 & 0 \end{vmatrix},$$

$\Delta_1, \Delta_2, \Delta_3, \Delta_4$ and Δ_5 are obtained by replacing 1st, 2nd, 3rd, 4th and 5th column by $[(M_1 - F_1), M_2, M_3, M_4, (M_5 + F_2)]'$ in Δ_0 and

$$\begin{aligned} M_1 &= -\left(\frac{b_1 f_2 + b_2 f_1 (\gamma^{*2} - \xi^2) + b_3 f_1 \gamma^{*2} - \tau_{11} f_3}{f_4} \right), \\ M_2 &= \frac{\iota b_3 \xi \gamma^* f_1}{f_4}, \quad M_3 = -\frac{\iota b_9 \xi f_2}{f_4}, \quad M_4 = \frac{b_{10} \alpha_0 \gamma^* f_2}{f_4}, \quad M_5 = -\frac{f_3}{f_4}, \\ b_1 &= \frac{\lambda_0}{\rho c_1^2}, \quad b_2 = \frac{\lambda}{\rho c_1^2}, \quad b_3 = \frac{2\mu + K}{\rho c_1^2}, \quad b_5 = \frac{\mu + K}{\rho c_1^2}, \quad b_6 = \frac{\mu}{\rho c_1^2}, \\ b_7 &= \frac{K}{\rho c_1^2}, \quad b_8 = \frac{\omega^{*2} \gamma}{\rho c_1^4}, \quad b_9 = \frac{\omega^{*2} b_0}{\rho c_1^4}, \quad b_{10} = \frac{\omega^{*2}}{\rho c_1^4}. \end{aligned}$$

Particular cases

(i) If we use $\tau_1 = \tau^1 = 0$, $\varepsilon = 1$ in Eqs. (4.3)–(4.7), the corresponding expressions of stresses, displacements and temperature distribution are obtained for microstretch thermoelastic half space with one relaxation time.

(ii) If we use $\varepsilon = 0$ in Eqs. (4.3)–(4.7), the corresponding expressions of stresses, displacements and temperature distribution are obtained for microstretch thermoelastic half space with two relaxation times.

(iii) Using $\tau^0 = \tau^1 = \tau_0 = \tau_1 = 0$ in Eqs. (4.3)–(4.7), yields the corresponding expressions of stresses, displacements and temperature distribution for microstretch coupled thermoelastic half space.

Special cases

Micropolar thermoelastic solid. In the absence of microstretch effect in Eqs. (4.3)–(4.7), the corresponding expressions of stresses, displacements and temperature are obtained for micropolar generalized thermoelastic half space.

Inversion of the transform

The transformed displacements, stresses and temperature changes are functions of the parameters of Laplace and Fourier transforms s and ξ respectively, and hence these have the form $f(s, \xi, z)$. To obtain the solution to the problem in the physical domain, we must invert the Laplace and Fourier transforms by using the method used by KUMAR [35].

5. Numerical results and discussions

In order to illustrate the theoretical results obtained in the preceding sections, some numerical results are presented. For numerical computation, the values for relevant parameters for microstretch thermoelastic medium following from ERINGEN [34] are $\lambda = 9.4 \times 10^{10} \text{ N} \cdot \text{m}^{-2}$, $\mu = 4.0 \times 10^{10} \text{ N} \cdot \text{m}^{-2}$, $K = 1.0 \times 10^{10} \text{ N} \cdot \text{m}^{-2}$, $\rho = 1.74 \times 10^3 \text{ Kg} \cdot \text{m}^{-3}$, $j = 0.2 \times 10^{-19} \text{ m}^2$, $\gamma = 0.779 \times 10^{-9} \text{ N}$. The microstretch parameters are taken as $j_0 = 0.19 \times 10^{-19} \text{ m}^2$, $\alpha_0 = 0.45 \times 10^{-9} \text{ N}$, $b_0 = 0.5 \times 10^{-9} \text{ N}$, $\lambda_0 = 0.92 \times 10^{10} \text{ N} \cdot \text{m}^{-2}$, $\lambda_1 = 0.5 \times 10^{10} \text{ N} \cdot \text{m}^{-2}$, $c^* = 1.04 \times 10^3 \text{ J} \cdot \text{Kg}^{-1} \cdot \text{K}^{-1}$, $K^* = 1.7 \times 10^2 \text{ J} \cdot \text{m}^{-1} \cdot \text{s}^{-1} \cdot \text{K}^{-1}$, $\alpha_{t1} = 2.33 \times 10^{-5} \text{ K}^{-1}$, $\alpha_{t2} = 2.48 \times 10^{-5} \text{ K}^{-1}$, $T_0 = 0.298 \times 10^3 \text{ K}$, $\tau_0 = 0.02$, $\tau_1 = 0.03$.

A comparison of the dimensionless form of field variables for the cases of microstretch thermoelastic medium with a laser pulse (MSTL), microstretch thermoelastic medium without a laser pulse (MST), micropolar thermoelastic medium with a laser pulse (MPL) and micropolar thermoelastic medium without a laser pulse (MP) subjected to normal force and thermal source is presented in Figs. 1–10. For all cases, the values of all physical quantities are shown in the range $0 \leq x_1 \leq 20$.

Solid lines and dash lines correspond to microstretch thermoelastic solid with a laser pulse (MSTL) and microstretch thermoelastic solid without a laser pulse (MST), respectively.

Solid lines with a central symbol and dash lines with a central symbol correspond to micropolar thermoelastic solid with a laser pulse (MPL) and micropolar thermoelastic solid without a laser pulse (MP), respectively.

The computations were carried out in the absence and in the presence of laser pulse ($I_0 = 10^5, 0$) and on the surface of plane $x_1 = 1, t = 0.1$.

I. Normal force

Figure 1 shows the variation of normal stress t_{33} with the distance x_1 . It can be noticed that the normal stress t_{33} shows a similar behavior for MSTL and MST. The value of normal stress for MSTL and MST monotonically increases as x_1 and then oscillates. The value of t_{33} increases near the place of application of normal force due to the stretch effect and then keeps oscillating for all the values of x_1 .

Figure 2 shows the variation of tangential stress t_{31} with the distance x_1 . It can be noticed that the behavior of t_{31} for MSTL and MST shows initially a similar trend, whereas t_{31} for MPL and MP exhibits opposite behavior. Initially, t_{31} decreases monotonically for MSTL and MST, whereas for MPL and MP the initial trend of tangential stress increases. The values of t_{31} for all the cases, remain oscillatory and approach the boundary surface away from the point of application of normal force.

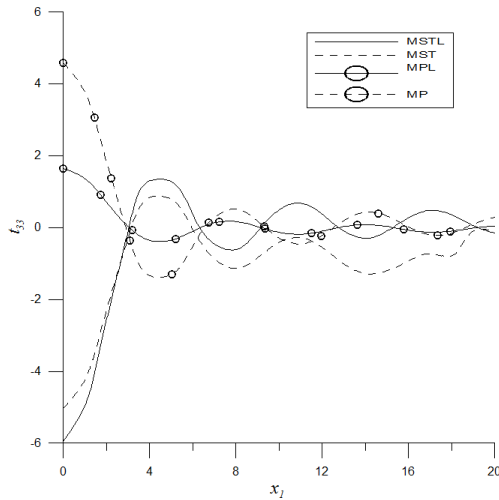


FIG. 1. Variation of t_{33} with distance.

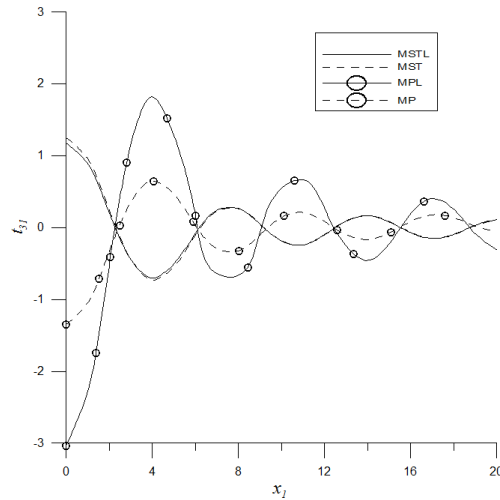


FIG. 2. Variation of t_{31} with distance.

Figure 3 shows the variation of couple stress m_{32} with distance x_1 for MSTL, MST, MPL and MP. The behavior and variation of m_{32} for (MSTL, MPL) and (MST, MP) remain opposite to each other for all the values of x_1 due to the effect of laser.

Figure 4 presents the variation of microstress λ_3^* with distance x_1 . The trend and variation of λ_3^* are similar to each other for both the cases, i.e., MSTL and MST.

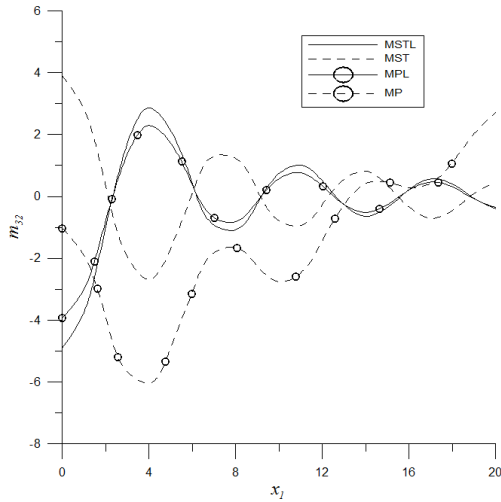
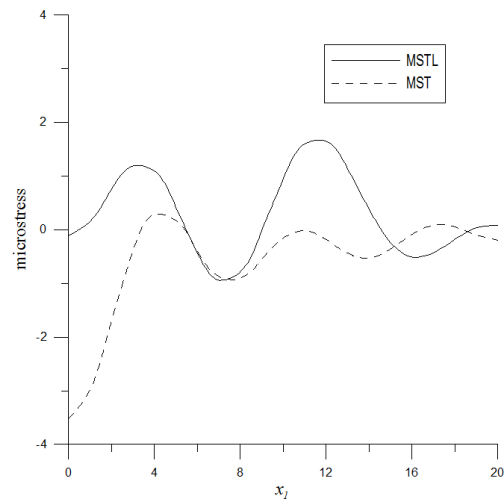
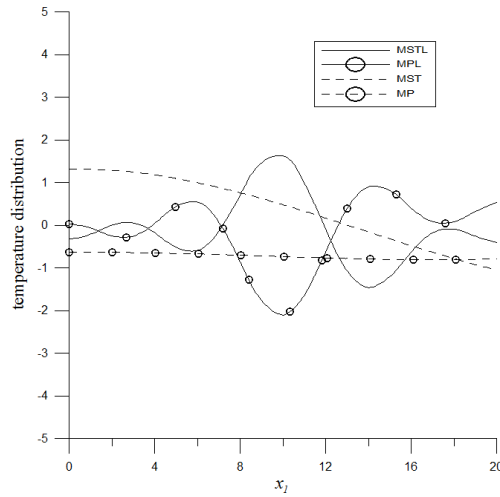
FIG. 3. Variation of m_{32} with distance.FIG. 4. Variation of λ_3^* with distance.FIG. 5. Variation of T with distance.

Figure 5 displays the variation of temperature T with distance x_1 . The values of temperature change for MSTL and MPL show an oscillatory trend while for MST and MP the temperature change shows a monotonically decreasing trend for all the values of x_1 .

II. Thermal source

Figure 6 shows the variation of normal stress t_{33} with distance x_1 . It can be noticed that t_{33} keeps oscillating for all the values of x_1 . Normal stress t_{33} approaches zero away from the source for all the cases considered.

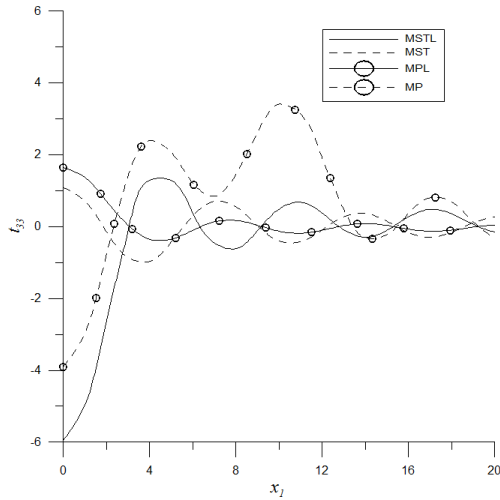


FIG. 6. Variation of t_{33} with distance.

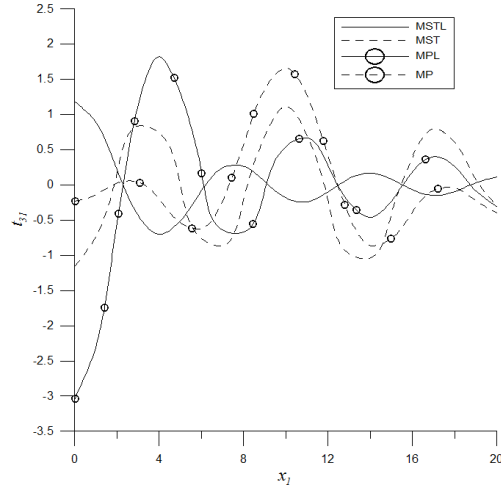


FIG. 7. Variation of t_{31} with distance.

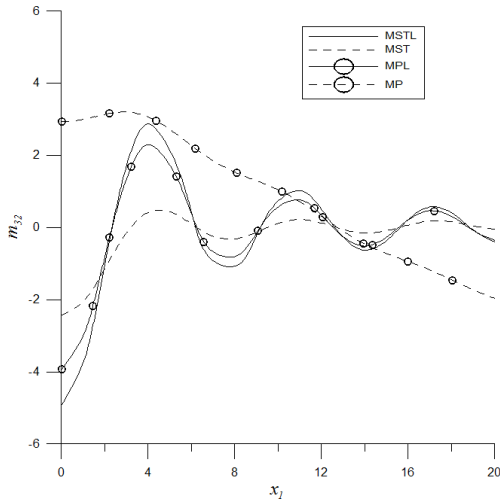


FIG. 8. Variation of m_{32} with distance.

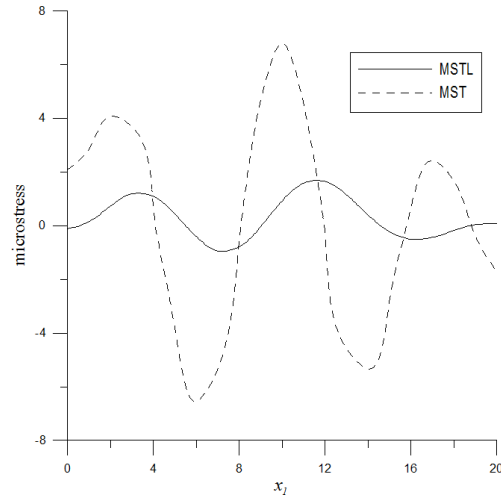


FIG. 9. Variation of λ_3^* with distance.

Figure 7 displays the variation of tangential stress t_{31} with distance x_1 . It can be noticed that initially the behavior of t_{31} for MST, MPL and MP shows a similar trend, whereas t_{31} for MSTL exhibits different behavior near the point of application of the source. The values of t_{31} for all the cases remain oscillatory and approach the boundary surface away from the source.

Figure 8 shows the variation of couple stress m_{32} with distance x_1 for MSTL, MST, MPL and MP. The behavior and variation of m_{32} for (MSTL, MPL, MST and MP) remain similar to each other for all the values of x_1 .

Figure 9 depicts the variation of microstress λ_3^* with distance x_1 . The trend and variation of λ_3^* are similar to each other for both the cases, i.e., MSTL and

MST. The variation in the value of λ_3^* for MSTL is smaller than the variation of λ_3^* for MST.

Figure 10 displays the variation of temperature T with distance x_1 . The values of temperature change for MSTL, MPL, MST and MP are similar. Temperature change tends to approach the boundary surface away from the source.

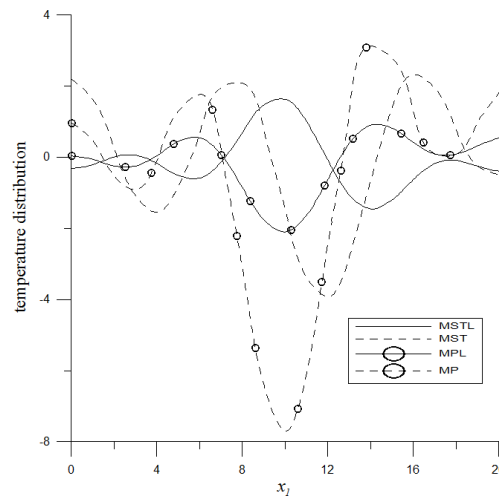


FIG. 10. Variation of T with distance.

6. Conclusions

The studied problem involves investigating displacement components, scalar microstretch, temperature distribution and stress components in a homogeneous isotropic microstretch thermoelastic half space due to various sources subjected to a laser pulse. The integral transform technique is employed to express the results mathematically. The theoretically obtained field variables are also exemplified through a specific model to present the results in the transformed domain.

The analysis of results leads to the following concluding remarks:

(1) It can be clearly seen in the figures that all the field variables have nonzero values only in the bounded region of space, what indicates that all the results are in agreement with the generalized theory of thermoelasticity.

(2) The effect of microstretch is much pronounced in all the resulting quantities.

(3) It can be noticed in the figures that the laser heat source plays a significant role in all the field quantities. A change in the value of I_0 causes significant changes in all the simulated resulting quantities.

(4) If the laser pulse and microstretch effect is neglected, then the results are obtained for generalized thermoelastic problem; the results are in agreement with ELHAGARY [30] after neglecting diffusion effect.

(5) The variation of microstress differs significantly due to the presence of normal force and due to the presence of thermal source.

(6) Tangential stress, couple stress and temperature change are also affected due to microstretch effect as well as load/source applied.

The new model is employed in a microstretch thermoelastic medium as a new improvement in the field of thermoelasticity. The subject becomes more interesting due to irradiation of a laser pulse with an extensive short duration or a very high heat flux. This has found numerous applications. The method used in this article is applicable to a wide range of problems in thermodynamics. With the obtained results, it is expected that the present model of equations will serve as more realistic model and will provide motivation to investigate microstretch generalized thermoelasticity problems regarding laser pulse heat with high heat flux and/or short time duration.

References

1. A.C. ERINGEN, *Linear theory of micropolar elasticity*, Journal of Mathematics and Mechanics, **15**, 909–923, 1966.
2. A.C. ERINGEN, *Micropolar elastic solids with stretch*, Ari Kitabevi Matbassi, **24**, 1–18, 1971.
3. A.C. ERINGEN, *Theory of thermomicrostretch elastic solids*, International Journal of Engineering Science, **28**, 12, 1291–1301, 1990.
4. S.D. CICCIO, *Stress concentration effects in microstretch elastic bodies*, International Journal of Engineering Sciences, **41**, 187–199, 2003.
5. M.A. EZZAT, E.S. AWAD, *Constitutive relations, uniqueness of solution, and thermal shock application in the linear theory of micropolar generalized thermoelasticity involving two temperatures*, Journal of Thermal Stresses, **33**, 3, 226–250, 2010.
6. R. KUMAR, T. KANSAL, *Fundamental solution in the theory of thermomicrostretch elastic diffusive solids*, ISRN Applied Mathematics, volume **2011**, Article ID 764632, 2011.
7. M. MARIN, *A domain of influence theorem for microstretch elastic materials*, Nonlinear Analysis: Real World Applications, **11**, 3446–3452, 2010.
8. M. AOUADI, *Thermomechanical interactions in a generalized thermomicrostretch elastic half space*, Journal of Thermal Stresses, **29**, 511–528, 2006.
9. M.I.A. OTHMAN, S.Y. ATWA, A. JAHANGIR, A. KHAN, *Gravitational effect on plane waves in generalized thermo-microstretch elastic solid under Green–Naghdi theory*, Appl. Math. Inf. Sci. Lett., **1**, 2, 25–38, 2013.
10. D. TRAJKOVSKI, R. CUKIC, *A coupled problem of thermoelastic vibrations of a circular plate with exact boundary conditions*, Mech. Res. Commun., **26**, 217–24, 1999.

11. X. WANG, X. XU, *Thermoelastic wave induced by pulsed laser heating*, Appl. Phys. A, **73**, 107–14, 2001.
12. X. WANG, X. XU, *Thermoelastic wave in metal induced by ultrafast laser pulses*, J. Thermal Stresses, **25**, 457–73, 2002.
13. D. JOSEPH, L. PREZIOSI, *Heat waves*, Rev. Mod. Phys., **61**, 41–73, 1989.
14. M.N. OZISIK, D.Y. TZOU, *On the wave theory in heat-conduction*, ASME J. Heat Transfer, **116**, 526–535, 1994.
15. W.S. KIM, L.G. HECTOR, M.N. OZISIK, *Hyperbolic heat conduction due to axisymmetric continuous or pulsed surface heat sources*, J Appl. Phys., **68**, 5478–85, 1990.
16. T.Q. QIU, C.L. TIEN, *Heat transfer mechanisms during short-pulse laser heating of metals*, ASME J. Heat Transfer, **115**, 835–41, 1993.
17. D.Y. TZOU, *Macro to Micro Scale Heat Transfer: The Lagging Behavior*, Bristol, Taylor & Francis, 1997.
18. J. WANG, Z. SHEN, B. XU, X. NI, J. GUAN, J. LU, *Simulation on thermoelastic stress field and laser ultrasound wave form in non-metallic materials by using FEM*, Applied Physics A, **84**, 301–307, 2006.
19. C.B. SCRUBY, L.E. DRAIN, *Laser Ultrasonics Techniques and Applications*, Adam Hilger, Bristol, UK, 1990.
20. L.R.F. ROSE, *Point-source representation for laser-generated ultrasound*, Journal of the Acoustical Society of America, **75**, 3, 723, 1984.
21. F.A. McDONALD, *On the precursor in laser-generated ultrasound waveforms in metals*, Applied Physics Letters, **56**, 3, 230–232, 1990.
22. J.B. SPICER, A.D.W. MCKIE, J.W. WAGNER, *Quantitative theory for laser ultrasonic waves in a thin plate*, Appl. Phys. Lett., **57**, 1882–1884, 1990.
23. M. DUBOIS, F. ENGUEHARD, L. BERTRAND, M. CHOQUET, J.P. MONCHALIN, Appl. Phys. Lett., **64**, 554, 1994.
24. M.A. EZZAT, A. KARAMANY, M.A. FAYIK, *Fractional ultrafast laser-induced thermoelastic behavior in metal films*, Journal of Thermal Stresses, **35**, 637–651, 2012.
25. N.S. AL-HUNITI, M.A. AL-NIMR, *Thermoelastic behavior of a composite slab under a rapid dual-phase-lag heating*, Journal of Thermal Stresses, **27**, 607–623, 2004.
26. J.K. CHEN, J.E. BERAUN, C.L. THAM, *Comparison of one-dimensional and two-dimensional axisymmetric approaches to the thermomechanical response caused by ultra-short laser heating*, Journal of Optics, **4**, 650–661, 2002.
27. W.S. KIM, L.G. HECTOR, R.B. HETNARSKI, *Thermoelastic stresses in a bonded layer due to repetitively pulsed laser heating*, Acta Mechanica, **125**, 107–128, 1997.
28. H.M. YOUSSEF, A.A. EL-BARY, *Thermoelastic material response due to laser pulse heating in context of four theorems of thermoelasticity*, Journal of Thermal Stresses, **37**, 1379–1389, 2014.
29. L. YUAN, K. SUN, Z. SHEN, X. NI, J. LU, *Theoretical study of the effect of enamel parameters on laser induced surface acoustic waves in human incisor*, Int. J. Thermophys., July 2014.

30. M.A. ELHAGARY, *A two-dimensional generalized thermoelastic diffusion problem for a thick plate subjected to thermal loading due to laser pulse*, Journal of Thermal Stresses, **37**, 1416–1432, 2014.
31. A.C. ERINGEN, *Microcontinuum Field Theories I: Foundations and Solids*, Springer, New York 1999.
32. H.W. LORD, Y. SHULMAN, *A generalized dynamical theory of thermoelasticity*, J. Mech. Phys. Solid, **15**, 299–306, 1967.
33. A.E. GREEN, K.A. LINDSAY, *Thermoelasticity*, Journal of Elasticity, **2**, 1–5, 1972.
34. A.C. ERINGEN, *Plane waves in non-local micropolar elasticity*, Int. J. Eng. Sci., **22**, 1113–1121, 1984.
35. R. KUMAR, L. RANI, *Elastodynamic response of mechanical and thermal source in generalized thermoelastic half space with voids*, Mechanics and Mechanical Engineering, **9**, 2, 29–45, 2005.

Received January 25, 2015; revised version October 17, 2015.
